A study of turbulence and cyclic variation levels in internal combustion engine cylinders

by

N. St.Hill, P. Asadamongkon and K.C. Lee

Experimental and Computational Laboratory for the Analysis of Turbulence
Mechanical Engineering Department
King's College London
Strand, London WC2R 2LS, U.K.

ABSTRACT

This paper describes an experimental investigation of the cyclic variations and instability of the jet flows in the cylinders of dual-intake port gasoline engines under both steady-state and motored engine conditions using laser-Doppler anemometry and spectral analysis techniques.

An experimental investigation of the cyclic variations and instability of the jet flows in the cylinders of dual-intake port gasoline engines under motored engine and steady-state conditions using laser-Doppler anemometry and spectral analysis techniques.

Cyclic variations within the cylinder of an internal combustion engine were investigated by comparing cycle-to-cycle variation and turbulence levels of a point near the centre of the cylinder to those of a point within the intake jet. The velocity spectra at these points were also analysed using spectral analysis techniques. Cyclic variation levels have also been shown to broaden the values of turbulence. Figure 1 shows a plot of mean velocity versus crank angle and displacement below a valve with the colour code denoting cyclic variation levels normalised with mean piston speed. It is clear that these levels are higher than 50% of the mean piston speed even near TDC compression.

The instability of the jet flows around the inlet valves was studied under steady state conditions by quantifying the values of skewness and kurtosis.
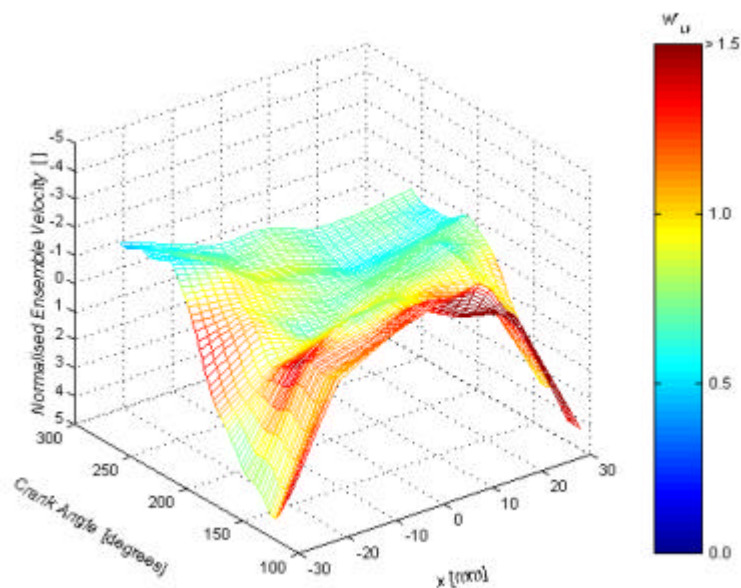
Figure 1: Normalised ensemble mean velocities and cyclic variation levels against crank angle and displacement (induction–compression).

1. INTRODUCTION

Analysis of the large scale (mean) and the small (turbulence) motions within an internal combustion engine are of paramount importance for the improvement engine performance. The effect of these motions on flame propagation, hence the performance and emissions characteristics in spark ignition engines has been studied by a number of researchers, for example, Fansler and French (1987).

Quantification of the characteristics such as mean velocity, turbulence and cycle-to-cycle variation levels is of particular relevance for the initiation of combustion and flame kernel growth. The turbulent and unsteady velocity field in an internal combustion engine is characterised by cycle-to-cycle variations at low frequencies and turbulence spread over the whole spectra (Sullivan *et al.*, 1999). Determination of cyclic variations and flow instabilities that may broaden the measured turbulence levels is thus essential. Findings of resent studies by others suggest that there are a number of factors that may influence the measured turbulence levels in engines and studies of the flows within motored engines have suggested swirl centre precession and cycle-to-cycle (Arcoumanis *et al.*, 1987; Suen 1992). Instabilities were found to occur even under steady flow conditions and the presence of vortex breakdown (Coghe, 1988) and vortex shedding (Hommersom *et al.*, 1989) have been suggested.

Flow instability under the intake ports of a dual-intake port gasoline engine (often termed jet flapping) can be studied under motored engine conditions by quantifying the cycle-resolved turbulence and cycle-to-cycle variation at individual locations within the cylinder. A number of techniques have been used to quantify these properties in engines previously. Catania and Mittica (1989) compared a number of techniques and suggested one of their own. Since their comparison there has been the arrival of the wavelet-based averaging techniques. There are now primarily three major techniques for quantifying mean and turbulence velocities: ensemble; cyclic (Catania and Mittica, 1989; Liou and Santavicca, 1985; Fansler and French, 1988 and Le Coz, 1992) and the new wavelet-based averaging (Wiktorsen *et al.*, 1996 and Sullivan *et al.*,1999). Sullivan *et al.* (1999) compared these averaging techniques and showed the strength of wavelet technique in its ability to compute turbulence without the need for the determination of a cut-off frequency, which is the down side of the cyclic techniques. However he also noted that the discrete wavelet transform technique suffered from the same subjectivity in implementation as the cyclic techniques because of the choice of the number of decompositions.

Most studies of the flow in internal combustion engines have concentrated on the in-cylinder flow due to the difficulties associated with the application of non-obtrusive optical techniques to complex geometries such as those of the inlet ports. These problems may be ameliorated by using a refractive index matching (RIM) technique in combination with laser-Doppler anemometry (LDA) (Nadarajah *et al,*1998).

In the present work LDA is used in combination with spectral analysis to study the flow within a motored engine cylinder with a transparent Pyrex liner. LDA and RIM techniques are also used to study instabilities within the inlet jet under steady flow conditions by determining the values of skewness and kurtosis of the probability distribution functions of the instantaneous velocities.
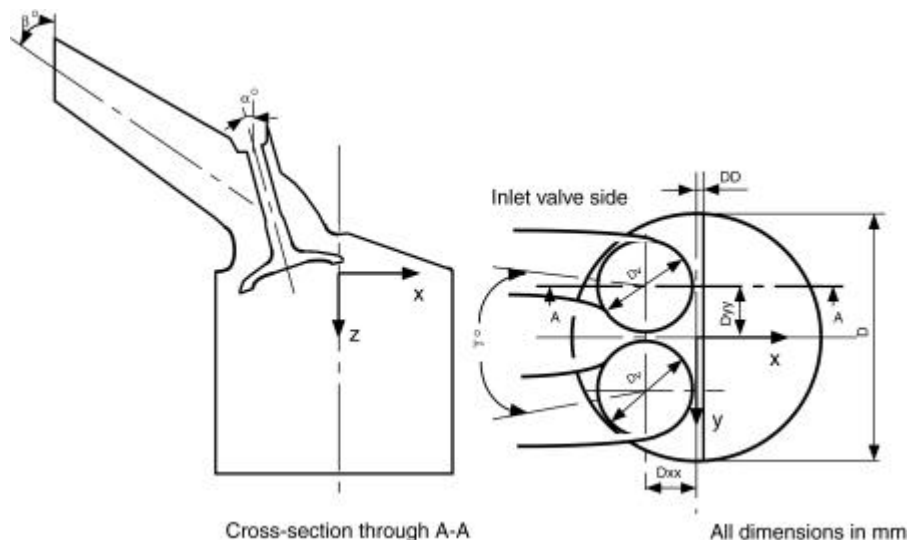

Figure 2: Elevation and plan view of engine inlet port and cylinder.

2. EXPERIMENTAL SETUP AND PROCEDURE

The major features of the motored engine and steady flow replica are shown in Figure 2, with their geometric specifications listed in Table 1. Both cylinder heads had directed inlet ports and pent-roof combustion chambers. The coordinate system employed is also shown in Figure 2.

Table 1: Geometrical specifications of the dual-intake ports.

Experimental rig	Steady Flow	Motored
Engine design	Cosworth	Zetec
Bore, D (mm)	86	80
Port angle, β (°)	57	65.8
Angle between ports, γ (°)	16	16
Inlet valve diameter, D_v (mm)	35	32
Inlet valve angle, α (°)	17	20
DD (mm)	3	2
Dxx (mm)	16.8	16.5
Dyy (mm)	19.3	17.6

2.1. Motored optical engine

A single cylinder motored optical engine equipped with the four valve cylinder head of a 1.8 litre Ford Zetec engine was seated on a Pyrex glass cylinder. The motor was driven by a direct current motor, which allows easy speed regulation. The engine was driven at a crank speed of 500±5 rpm for most of the experiments; however extensive tests were also carried out at higher speeds in order to establish the scaling of the flow with speed. The main operating characteristics of the motored engine are shown in Table 2.

The use of a Pyrex glass cylinder allowed optical access throughout the cylinder. The working fluid was air seeded with silicon oil particles. Seeding was accomplished by passing the incoming air through a filter and then a set of atomisers, while maintaining the input gauge pressure at 1.5 bar. The seeding air pressure was then reduced to atmospheric pressure by passing it through a mixing chamber before entering the intake port of the engine. A schematic diagram depicting the seeding process is shown in Figure 3.

An optical incremental shaft encoder that provides a train of 1000 pulses per revolution was attached to the crankshaft. This encoder was used to monitor crankshaft speed and position. In order to differentiate TDC compression from TDC induction, an optical interrupter was mounted on the camshaft. The encoder and interrupter signals were fed to the Burst Spectrum Analyser (BSA) and used as an external clock and reset, respectively.

In-cylinder pressure was monitored by means of a Kistler electric pressure transducer (type 601A) and a charge amplifier (type 5001). The transducer was mounted in the position of the spark plug with the tip flush with the top of the pent roof chamber, so as not to impede the flow. A measurement range of 0—20 bar was used.

Table 2: Operating characteristics of motored engine.

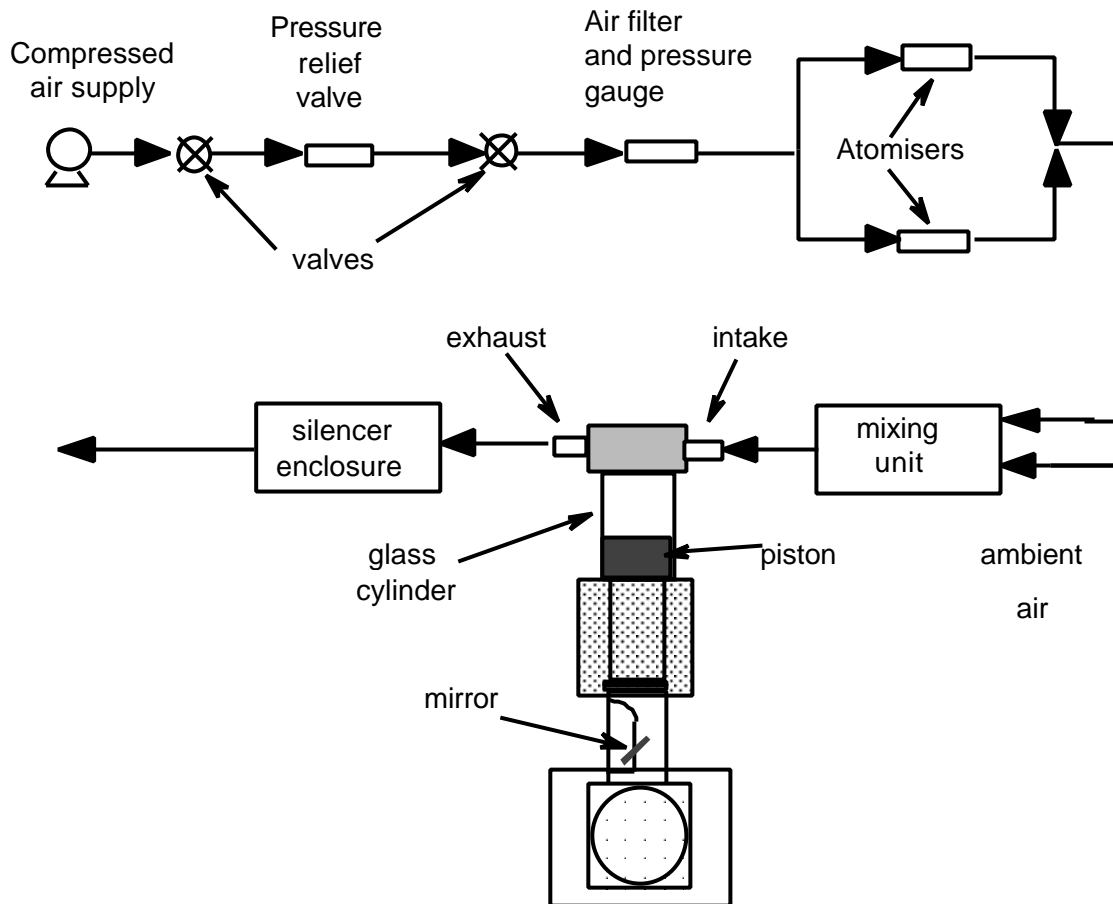|	
Displacement	1796 cc
Bore	80 mm
Stroke	90.0 mm
Compression Ratio	10.0 : 1
Inlet valve diameter	32.0 mm
Exhaust valve diameter	28.0 mm
Inlet valve opening	6 ° BTDC
Inlet valve closing	222 ° ATDC

Figure 3: Schematic of motored engine rig seeding process.

2.2. Steady flow rig

A CNC machine was used to manufacture a replica of a Cosworth engine port and cylinder from a clear cast acrylic plastic (Perspex) block; and the valves from Perspex rod accurately. A detailed description of the steady flow rig is given in Asadamongkon (2000).

The working fluid was a mixture of oil of turpentine and tetraline in a volume ratio of 69.2:32.8, which has an identical refractive index to that of Perspex at 24°C. In order to ensure accurate matching of the refractive indices of the working fluid and the Perspex, the temperature of the fluid mixture was controlled by a Proportional-integral (PI) temperature control system, which maintained the temperature at 24 ± 0.5 °C throughout the experiments.

A valve lift of 9 mm was used for both valves throughout the experiments, with a liquid mass flow rate of 3.06 kg/s, corresponding to a Reynolds number, based on the hydraulic diameter of the inlet port, of 60753.

The geometrical similarities of the motored engine and steady flow replica allow comparisons of the flows to be made, but clearly shape differences may have important influences and such comparisons must be made with care.

2.3. Measurement technique

The principal characteristics of the LDA systems used are listed in Table 3. Both LDA systems were operated in the forward scatter dual-beam mode. A diffraction grating was used to split the laser beam as well as provide the required frequency shift between the two first order beams. Instantaneous velocity signals were measured using

the BSA (Dantec, model 57N21 master). The quality of the Doppler signals was monitored continuously by means of an oscilloscope and the data and validation rates were monitored online, on the computer screen. Arrival rates as high as 40 kHz were obtained in the motored engine rig, and in general this was found to be sufficient to determine time-resolved turbulence levels during individual engine cycles.

For the steady flow skewness and kurtosis results presented, data were obtained from 10000 validated samples at a data rate of approximately 8.5 kHz.

Table 3: Principal characteristics of the laser Doppler anemometry systems.

Experimental rig	Steady Flow	Motored
Laser	He-Ne	Argon-ion
Wavelength, λ (nm)	632.8	514.5
Power (mW)	10	1000
Expanded beam diameter (at e^{-2} intensity) (mm)	0.83	1.1
Half-angle between incident beams(°)	4.27	4.85
Intersection volume diameter (at e^{-2} intensity), (μm)	77	120
Intersection volume length (at e^{-2} intensity), (μm)	1043	1140
Stationary fringes within the e^{-2} intensity level	19	48
Frequency to velocity conversion factor (m/s/MHz)	4.3	6.1
Frequency shift (MHz)	3.6	5.46

2.4. Motored engine data treatment

In this work, the data was processed using a low pass filter, to differentiate between cyclic variation and turbulence following a similar principle as employed in Fansler and French (1988). The relationships used to quantify the values of ensemble mean velocities, turbulence levels and cycle-to-cycle variations are described below to clarify the terms employed.

The ensemble-averaged angle-resolved mean velocity of N valid cycles at crank angle q is given by:

$$\langle U(q) \rangle = \frac{1}{N_v(q)} \sum_{i=1}^{N} U(q, i)$$
(1)

where $N_v(q)$ is the total number of valid velocity estimates at crank angle interval q over all N cycles, for each cycle i and

$$U(q, i) = \langle U(q) \rangle + u(q, i)$$
(2)

where $U(q,i)$ is the instantaneous velocity and $u(q,i)$ is the fluctuating velocity.

On filtering, the fluctuating velocity may be separated into low and high frequency components:

$$U(q, i) = \langle U(q) \rangle + u_{LF}(q, i) + u_{HF}(q, i)$$
(3)

The filtered in-cycle mean velocity is the sum of the ensemble-averaged mean and the low frequency fluctuation:

$$U_{LF}(q, i) = \langle U(q) \rangle + u_{LF}(q, i)$$
(4)

$$\langle U_{LF} \rangle = \langle U \rangle$$
(5)

The intensities of the high and low frequency fluctuations can be characterised by their variances about appropriate mean velocities.

$$u_{HF} = \sqrt{\langle u_{HF}^2 \rangle} = \sqrt{\langle (U - U_{LF})^2 \rangle}$$
(6)

$$u'_{LF} = \sqrt{\left\langle u_{LF}^2 \right\rangle} = \sqrt{\left\langle \left(U_{LF} - \langle U \rangle \right)^2 \right\rangle} \qquad (7)$$

The ensemble-averaged rms fluctuation intensity u' is related to the low and high frequency fluctuations by

$$u' = \sqrt{\left\langle \left(u_{LF} + u_{HF} \right)^2 \right\rangle} \qquad (8)$$

where u'_{HF} is referred to as the turbulence level, and u'_{LF} is referred to as the cyclic variation of the mean.

The instantaneous velocity for each cycle is lowpass filtered using a Hamming filter. A characteristic of a Hamming filter is its flat response in the pass band and steep drop-off. These filters also have a known maximum gain of –50dB in the stop band. The frequency response of the filter is shown in Figure 4, with *fp* and *fs* representing the normalised passband and stopband frequencies, respectively. A cut-off frequency of 250 Hz and sampling frequency of 16.6 kHz was used. The cut-off frequency selected is approximately the maximum frequency in the spectra of the ensemble-mean velocity. A number of other cut-off frequencies were chosen above and below this value. The turbulence levels variation with a variation of ±100 Hz about the chosen cut-off frequency was found to be negligible.
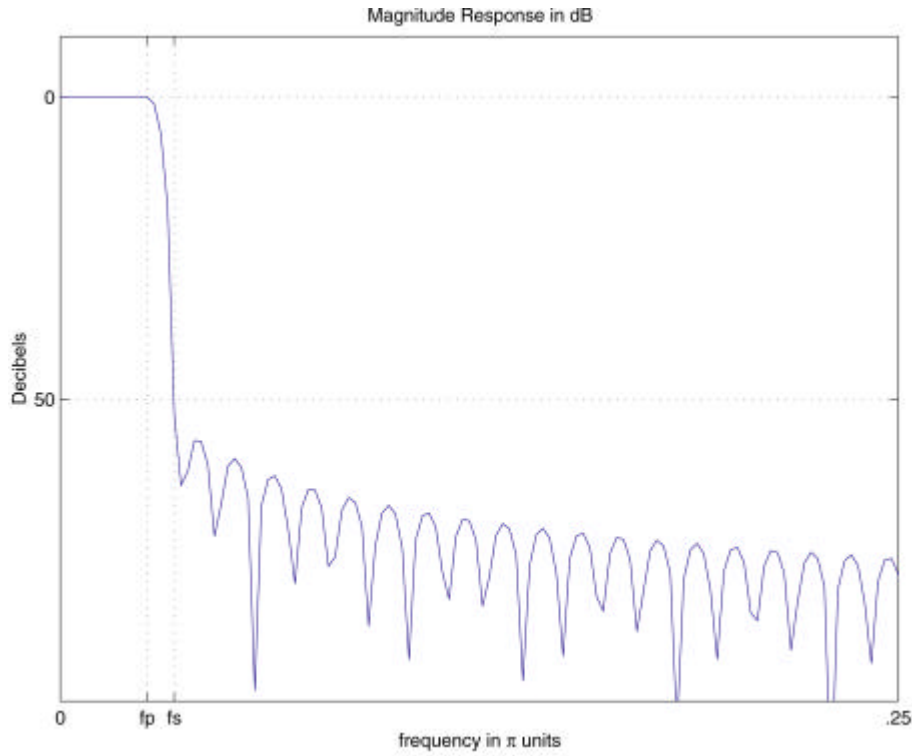

Figure 4: Frequency response of low pass filter.

Data was recorded during the induction and compression strokes. Linear interpolation was used for any missing data points during the gating period. Cycles which less than 95% of the required data were discarded. Instantaneous velocity fluctuations that were higher than three times the rms fluctuations were discarded. Mean velocity, turbulence levels and cycle-to-cycle variation levels were calculated with sample sets where at least 95% of the data were within the ±3*s* range.

3. RESULTS AND DISCUSSION

3.1. Motored engine

Ensemble-averaged rms, cycle-resolved turbulence and cycle-to-cycle variation

The variations of the axial (in the z-direction) ensemble-averaged rms (w'), the cycle-resolved turbulence (w'_{HF}) and cycle-to-cycle variation (w'_{LF}) with crank angle during induction and compression are presented in Figures 5(a) and (b). Figure 5(a) shows the results obtained at a location near the centre of the cylinder, and Figure 5(b) shows the results obtained at a location within the inlet jet. All motored engine results are normalised with the mean piston speed V_p.

It can be observed from Figures 5(a) and (b) that the turbulence levels (both w'_{LF} and w'_{HF}) are higher during induction within the intake jet region, as might be expected. Cyclic variation levels are substantial at both locations, but more significant near the centre of the cylinder. In general the w'_{LF} variation with crank angle is found to be similar throughout the cylinder. During compression the w', w'_{HF} and w'_{LF} levels decrease and remain fairly constant. It is clear from Figure 5 that the w' levels may overestimate the amount of *'true'* turbulence w'_{LF} by as much as 100% in many parts of the cycle.

Figures 6(a) and (b) show the variation of turbulence and cycle-to-cycle variation levels with crank angle and displacement along the x-axis at $y = -17.6$ mm and $z = 30$ mm. The trends noted in Figure 5 can still be observed. Throughout the axis, cycle-to-cycle variation levels are found to be greater than the turbulence levels as TDC compression is approached.
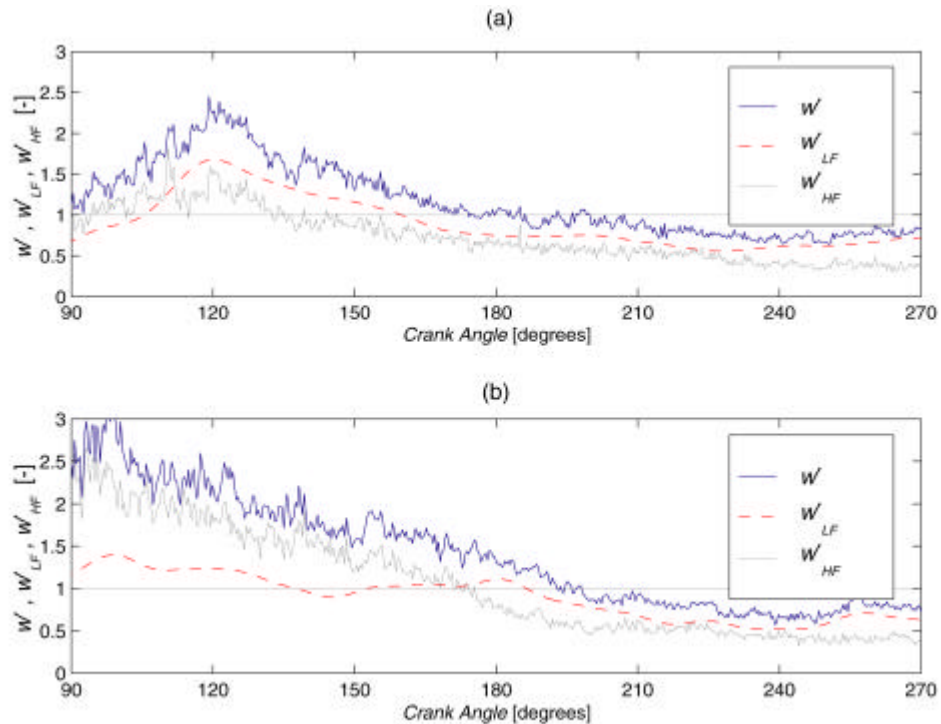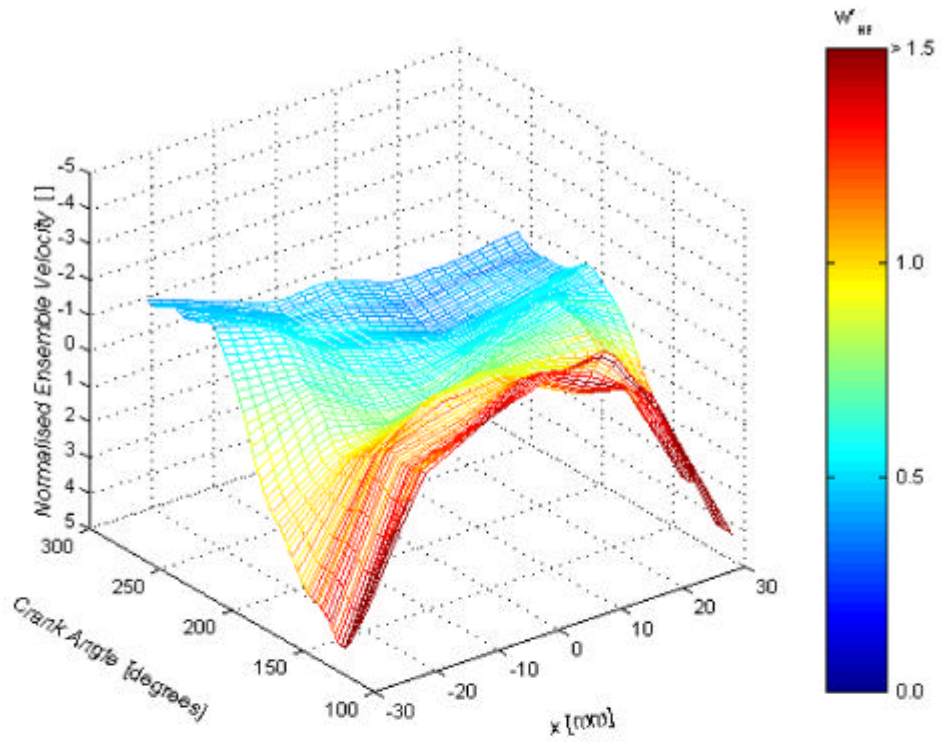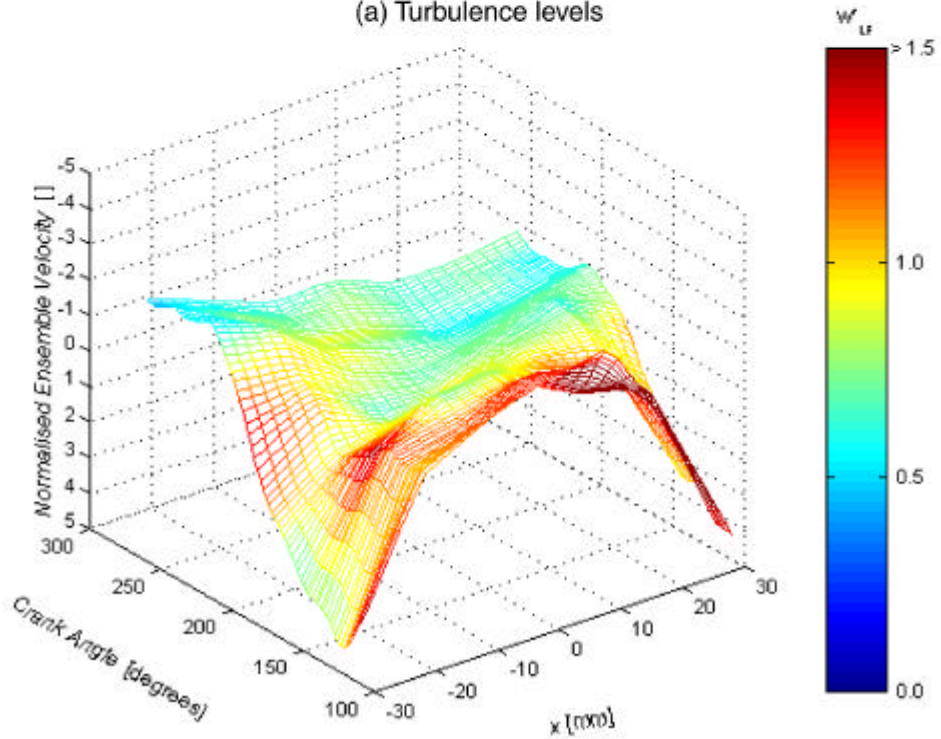

Figure 5:   Crank-angle ensemble averaged RMS, cycle resolved turbulence and cyclic variation
(a)   x = 10 mm, y = -17.6 mm and z = 30 mm; and
(b)   x = 30 mm, y = -17.6 mm and z = 30 mm.

(a) Turbulence levels

(b) Cycle-to-cycle variation levels

Figure 6: Comparison of turbulence and cycle-to-cycle variation levels with variation of crank angle and displacement along the y = -17.6 mm and z = 30 mm axis.

3.2. Spectral analysis

Figures 7(a) and (b) show the *W*-velocity spectra obtained at the same locations as in Figure 6, i.e. at $x = 10$ mm, $y = -17.6$ mm, $z = 30$ mm and $x = 30$ mm, $y = -17.6$ mm, $z = 30$ mm, respectively. The frequencies of the six most significant peaks are indicated, and found to be multiples of the cam rotational frequency of 4.16 Hz, which may suggest that they are harmonics of the cam frequency. It can be seen from the figure that, the velocity spectrum at a location near the centre of the cylinder (Figure 7(a)) contains a broader band of significant peaks than that within the jet (Figure 7(b)).
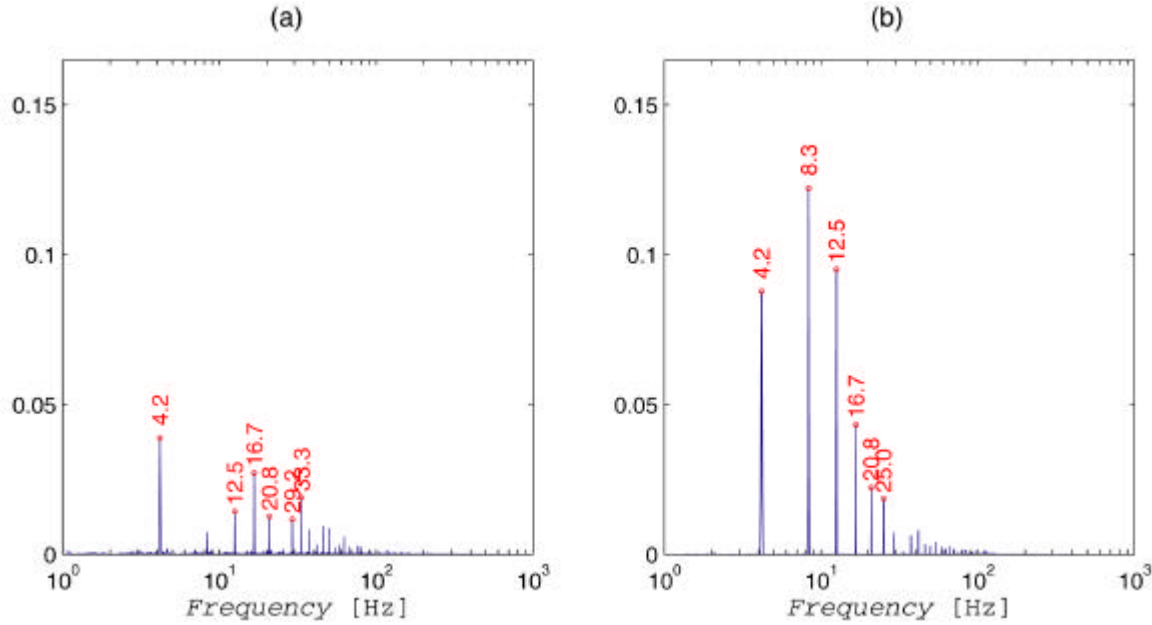

Figure 7: Normalised W-velocity power spectra at
(a) x = 10 mm, y = 17.6 mm and z = 30 mm; and
(b) x = 30 mm, y = 17.6 mm and z = 30 mm.

Mean velocity variation with number of samples and number of cycles

The high levels of cyclic variation noted above raise the question of the number of samples/cycles required to obtain a representative velocity measurement in an engine. Results were found not to be as repeatable near the centre, as in other regions of the cylinder. Figure 8(a) shows the variation of the mean velocity with the number of samples at $x = 10$ mm, $y = -17.6$ mm and $z = 30$ mm. Large variations of the measured mean velocity with the number of samples are observed for sample sizes less than around 12000 (therein by more than 20 % of the mean piston speed, V_p, at a crank angle of 102.6°). These variations decrease to less than 0.05 V_p for 12000-18000 samples and thus indicate that great care must be exerted when selecting sample size in regions with high w'_{LF} and w'_{HF} levels.

Figure 8(b) shows the variation of the mean velocity with the number of cycles obtained at the same location as Figure 8(a). Again large variations of the W/V_p are noted when less than 200 cycles contribute to the measurement. For more than 300 cycles the results at the three crank angles presented have attained a variation in their ensemble mean velocities of less than 0.05 V_p. The results presented above indicate clearly that conventional ensemble-averaging techniques, even when use over a small crank angle interval (0.36° in the present work), may result in erroneous estimates of the mean velocity and turbulence levels in the motored engines.
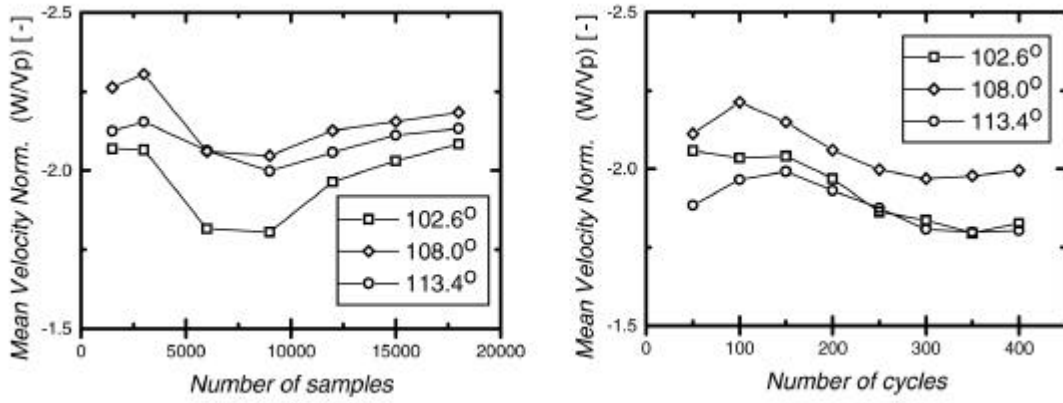
Figure 8: Mean velocity variation with (a) the number of samples and (b) the number of cycles.

3.3. Steady flow tests

In view of the aforementioned high w'_{LF} levels, it is important to understand the origin(s) of such variations, in order to identify means for their control and to predict engine performance better. This is a very complex task, but inlet jet flapping or flow instability may be one such possible source of variation (Nadarajah *et al,* 1998). For this reason, measurements of the predominant velocity component in the *x*-direction were made under steady flow conditions within the intake jet. Useful indications of possible jet instability are the third and the fourth moment of the velocity probability distribution function (pdf) (Tennekes *et al,*1972); these were calculated from the data and skewness (*S*, normalised by s^3) and kurtosis (*K*, normalised by s^4) profiles are shown in Figure 9. Gaussian distributions have *S* and *K* values of 0 and 3, respectively: deviation from such values might imply jet flapping/instability (Nadarajah *et al,* 1998). This is indeed the case in the data of Figure 9: maximum *K* and *S* values of 6.9 and -1.7 are observed near the centre of the jet. These indicate that the velocities are intermittently reduced in magnitude, which is consistent with the presence of jet flapping. Conversely, positive *S* values on either side of the jet centre indicate the velocity is skewed to lower values on the jet edges, again confirming the above indication of flapping. Evidence of such instability was also observed from light sheet flow visualisation, a characteristic sample of which is presented in Figure 10. The jet on the LHS of the valve shown indicated large direction variations with time. Spectral analysis of the steady flow velocity data also indicated a number of peaks, similar to those in Figure 7, which might also point to flow instability (Nadarajah *et al*., 1998).
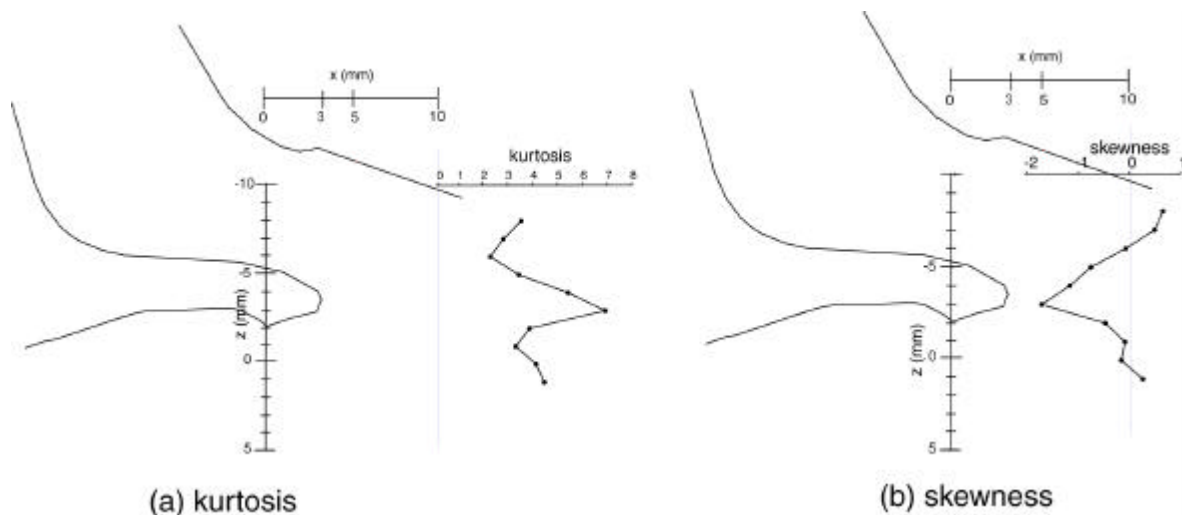

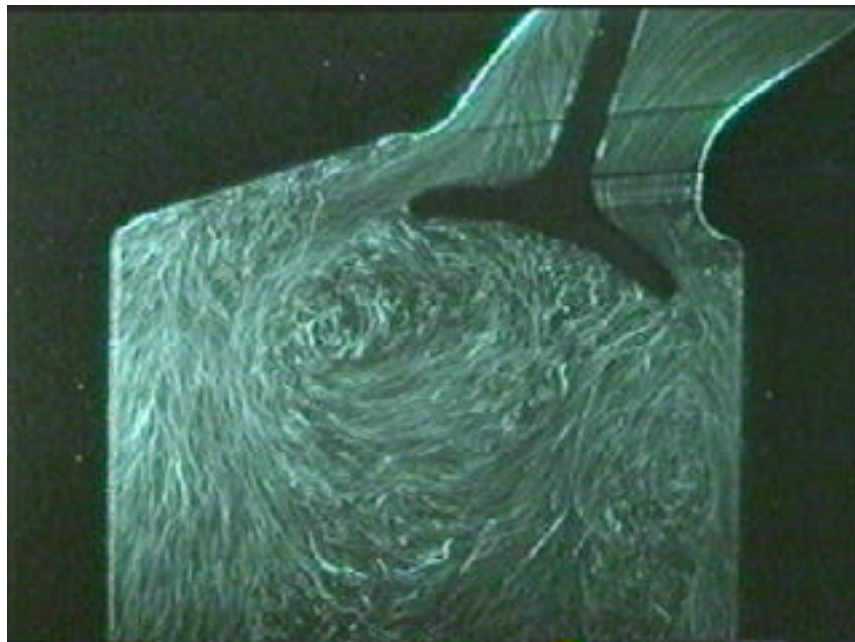*Figure 9: Profiles of skewness and kurtosis at x = 10 mm with 9 mm valve lift.*

Figure 10: Flow visualisation in the y = -19.3 mm plane.

4. CONCLUDING REMARKS

The data presented above show clearly that cyclic variation (due to the variation of the mean velocity from one cycle to the next) may be substantial in reciprocating engines; it can result in an overestimation of true turbulence levels by as much as 100% and must be taken into consideration when assessing engine turbulence levels and related CFD predictions. The origins of such high variations are not clearly understood, but analysis of steady flow data suggests that intake jet flapping may be one possible source. The complexity of the 3-D turbulence processes in engines makes identification of these origins a most challenging task, but work is in progress to obtain more extensive data and analysed their spectral content in more detail so as to improve understanding and help improve combustion and engine performance.

5. REFERENCES

Arcoumanis, C., Hadjiapostolou, A. and Whitelaw, J. H. (1987). "Swirl center precession in engine flows", SAE 870370

Asadamongkon, P. (2000). "An experimental study of steady flow through a generic dual-intake port engine", Ph.D. Thesis, King's College London, University of London. (in preparation)

Baby X. and Floch A. (1997) ."Investigation of the in-cylinder tumble motion in a multi-valve engine: Effect of the piston shape", SAE 971643.

Catania, A.E. and Mittica, A. (1989). "Extraction techniques and analysis of turbulence quantities from in-cylinder velocity data", ASME.

Coghe, A., Brunelo, G., and Tassi, E. (1988). "Effect of intake ports on the in-cylinder air motion under steady flow conditions", SAE 88034.

Fansler T.D. and French D.T. (1987). "Swirl, squish and turbulence in stratified charge engines: LDA measurements and implications for combustion", SAE Tech. Rep. 870371.

Fansler T.D. and French D.T. (1988). "Cycle-resolved laser-velocimetry measurements in a reentrant-bowl-in-piston engine", SAE 880377.

Hommersom, G., Evers, D. J. W. M. and Huigen, G. (1989). "Swirl generation by a directed inlet port of a diesel automotive engine under steady flow conditions", 3rd Int. Conf. On laser anemometry: advances and applications, University College of Swansea, 26-29 September, pp. 23.1-23.15.

Le Coz J.F. (1992). "Cycle to cycle correlation between flow field and combustion initiation in an S.I. engine", SAE 920517.

Liou T.-M. and Santavicca D.A. (1985). "Cycle resolved LDV measurements in a motored IC engine", Journal of Fluids Engineering, vol 107.

Nadarajah, S., Balabani, S., Tindal, M. J. and Yianneskis, M. (1998). "The turbulence structure of the annular non-swirling flow past an axisymmetric poppet valve", Proc. Instn Mech. Engrs, Part C, Journal of Mechanical Engineering Science, 212(C6), 455-471

Suen, K. O. (1992). "Investigation of gas flow in a motored high speed diesel engine by Laser-Doppler anemometry", Ph.D. thesis, King's College London, University of London.

Sullivan, P., Ancimer, R., and Wallace, J. (1999), "Turbulence averaging within spark ignition engines", Experiments in Fluids, Vol.27, No.1, pp.92-101.

Tennekes, H. and Lumley, J.L. (1972). A first Course in Turbulence, M.I.T. Press, Cambridge, Mass.